Journal of Magnetism and Magnetic Materials 400 (2016) 271–275

Contents lists available at ScienceDirect

Journal of Magnetism and Magnetic Materials

journal homepage: www.elsevier.com/locate/jmmm

Magnetic properties, morphology and interfaces of $(Fe/Si)_n$ nanostructures

J. Bartolomé [a,b,*], L. Badía-Romano [a,b], J. Rubín [a,c], F. Bartolomé [a,b], S.N. Varnakov [d], S.G. Ovchinnikov [d], D.E. Bürgler [e]

[a] *Instituto de Ciencia de Materiales de Aragón, CSIC-Universidad de Zaragoza, E-50009 Zaragoza, Spain*
[b] *Departamento de Física de la Materia Condensada, Universidad de Zaragoza, E-50009 Zaragoza, Spain*
[c] *Departamento de Ciencia de Materiales e Ingeniería Metalúrgica, Universidad de Zaragoza, E-50018 Zaragoza, Spain*
[d] *Kirensky Institute of Physics SB of RAS, 660036 Krasnoyarsk, Russia*
[e] *Peter Grünberg Institute (PGI-6), Forschungszentrum Jülich GmbH, D-52425 Jülich, Germany*

ARTICLE INFO

Article history:
Received 20 June 2015
Received in revised form
3 July 2015
Accepted 14 July 2015
Available online 16 July 2015

ABSTRACT

A systematic study of the iron–silicon interfaces formed upon preparation of (Fe/Si) multilayers has been performed by the combination of modern and powerful techniques. Samples were prepared by molecular beam epitaxy under ultrahigh vacuum onto Si wafers or single crystalline Ag(100) buffer layers grown on GaAs(100). The morphology of these films and their interfaces was studied by a combination of scanning transmission electron microscopy, X-ray reflectivity, angle resolved X-ray photoelectron spectroscopy and hard X-ray photoelectron spectroscopy. The Si-on-Fe interface thickness and roughness were determined to be 1.4(1) nm and 0.6(1) nm, respectively. Moreover, determination of the stable phases formed at both Fe-on-Si and Si-on-Fe interfaces was performed using conversion electron Mössbauer spectroscopy on multilayers with well separated Si-on-Fe and Fe-on-Si interfaces. It is shown that while a fraction of Fe remains as α-Fe, the rest has reacted with Si, forming the paramagnetic FeSi phase and a ferromagnetic Fe rich silicide. We conclude that there is an identical paramagnetic c-$Fe_{1-x}Si$ silicide sublayer in both Si-on-Fe and Fe-on-Si interfaces, whereas an asymmetry is revealed in the composition of the ferromagnetic silicide sublayer.

1. Introduction

In recent years multilayer magnetic structures have found many applications. Giant magnetoresistance was the starting point in Fe/Cr multilayers [1,2]. The field of spintronics is based on the artificial creation of nanostructures of ferromagnetic metal/semiconductor materials [3,4]. The injection of spin-polarized carriers from the ferromagnetic into a semiconductor one may be applied in spintronic devices with increased data processing speed, nonvolatility, lower power consumption and increased integration densities [5–7]. The interaction between ferromagnetic layers is one of the parameters governing the device function. Since the first observation of antiferromagnetic coupling between Fe layers separated by Cr [8] the control of this interaction has been a scientific goal of paramount importance.

The Fe/Si multilayers present a particularly interesting study platform since they are quite compatible with Si technology, and offer the case of alternating metal and non-metal layers with ferromagnetic [9] or antiferromagnetic [10] coupling between the metallic layers. The Si layer was found to have a relevant effect since the Fe–Fe interlayer exchange coupling (IEC) may show oscillatory character [11] or exponential dependence for increasing thickness [12]. The interface between the Fe and Si layers is not abrupt. It actually contains Fe silicides that may be ferro- or paramagnetic at room temperature. Their magnetic properties actually may have a strong detrimental effect in the spin carrier transport.

The Fe/Si interfaces have been studied in the last decades intensively. The composition of the interface silicides reported includes $FeSi_2$ [13–16], FeSi [13,17,18], Fe_2Si [19–21], Fe_3Si [22–25] at the Fe-on-Si interface, however in the Si-on-Fe one the presence of the paramagnetic c-$Fe_{1-x}Si$ is reported [17,22,26,27] while other authors assert that a ferromagnetic Fe-rich phase appears [19,20,25]. Besides, the Fe-on-Si and the Si-on-Fe interfaces seem to be different in composition since the Fe diffusion in Si is larger [16,17,19,22,28–30].

In the present paper recent results on the magnetic properties

---

[*] Corresponding author at: Instituto de Ciencia de Materiales de Aragón, CSIC-Universidad de Zaragoza, E-50009 Zaragoza, Spain.
E-mail address: barto@unizar.es (J. Bartolomé).

http://dx.doi.org/10.1016/j.jmmm.2015.07.046
0304-8853/© 2015 Elsevier B.V. All rights reserved.

of multilayers with an odd number of Fe/Si bilayers as well as the Fe-on-Si and Si-on-Fe interfaces studied with a combination of scanning transmission electron microscopy, X-ray reflectivity, angle resolved X-ray photoelectron spectroscopy, hard X-ray photoelectron spectroscopy and conversion electron Mössbauer spectrometry are reviewed with the aim to clarify the knowledge on the morphology, composition and structure of the Fe/Si interfaces.

2. Sample preparation

From the above review of results it was evident that the preparation method of the samples could affect the composition of the interfaces. In this work two sets of samples have been fabricated; Type A samples: molecular beam epitaxy (MBE) with thermal evaporation in vacuum on a Si substrate was used in the fabrication process. The thermal evaporation was performed at room temperature in an Angara type set up with a chamber pressure of 10^{-9} mbar. The substrates used were Si(100) and Si(111). The quality of the samples were checked in-situ by ellipsometry, Auger electron spectroscopy and energy-loss spectroscopy (EELS) [30,31]. In some samples a thin ^{57}Fe (0.6 nm) probe layer was deposited at determined depths tailoring the samples for conversion electron Mössbauer spectroscopy (CEMS). Type B samples: MBE using electron beam evaporators was applied to evaporate Fe or Si at a chamber pressure better than 10^{-9} mbar on a previously prepared single crystalline GaAs(001)/Fe/Ag(100) substrate, which is expected to yield improved crystallinity and reduce roughness [32]. The description of the morphology of each sample is given below in detail for each section.

2.1. Type A samples

The Type A samples Si(substrate)/[Fe(5 nm)/Si(2 nm)]$_n$/Fe(x)/Si(10 nm), with $n=2$–9, and $x=5$ and 10 nm, were prepared for magnetization and small-angle X-ray scattering measurements [30]. A decrease in the total magnetization and effective exchange coupling were explained to be caused by the formation upon deposition of magnetic silicides with lower magnetization than α-Fe [33]. To investigate the influence of the thickness of individual Fe layers Type A samples Si(hkl)/SiO$_2$/[Fe(x)/Si(1.5 nm)]$_2$/[Fe(x)/Si(10 nm)], with Si(hkl)=Si(100) and Si(111), and $x=1.2$, 1.6, 2.6 and 3.8 nm, were synthesized and their magnetization measured from 5 to 400 K [34]. It was found that the magnetization and exchange constant decrease with the thickness of the Fe layer, essentially due to the Fe silicide interface formation; i.e. the thinner the nominal layer, the more noticeable the size effect. When the same samples were annealed up to 800 K a change in the measured *in situ M(T)* slope at $T\approx 400$ K indicated that a second process of chemical reaction between the as-deposited Fe and Si was taking place till destruction of any α-Fe, when deposited on Si(111), and incomplete reaction of the available α-Fe when deposited on Si(100) substrate (see Fig. 1 left) [35]. Moreover, the Fe/Si chemical reaction was monitored in-situ as a function of time to relate it with the Fe/Si interdiffusion. The growth of the FeSi interlayer with increasing temperature above 400 K was monitored with temperature dependent cross-sectional transmission electron microscopy (TEM) [36].

The Fe layers deposited in Type A samples are ferromagnetic, with the easy axis contained in the Fe film plane, as could be expected for these very thin Fe films. It was unexpectedly observed that they show in-plane anisotropy [37]. The deposition direction forms an azimuthal angle with the normal to the substrate. In the case of deposition on a Si(100) substrate preoxidized with a SiO$_2$ buffer layer (Si(100)/SiO$_2$(1.5 nm)/Fe(10 nm)), local magnetization hysteresis measurements detect an in-plane easy magnetization direction *perpendicular* to the incoming flux plane. Evidently, it is not correlated to the substrate crystallographic plane, but instead it is associated to an anisotropic surface roughness formed during deposition. The sample lacking the SiO$_2$ buffer layer (Si(100)/Fe(10 nm)) presents two orthogonal easy axes of magnetization, corresponding to the two equivalent directions [110]Si and [−110] Si of the Si film. Thus, the epitaxial growth of the Fe film on the Si crystal dominates the deposition process in absence of the buffer layer. However, evidence of Fe silicide formation was also proven by a reduction of the effective magnetization of the Fe film.

To determine the morphology of the Si-on-Fe interface an *ad hoc* sample was synthesized, namely, Si(100)/SiO$_x$/Fe(20 nm)/Si(4.3 nm), where the SiO$_x$ is a naturally oxidized buffer. High Angle Annular Dark Field (HAADF) combined with electron energy loss

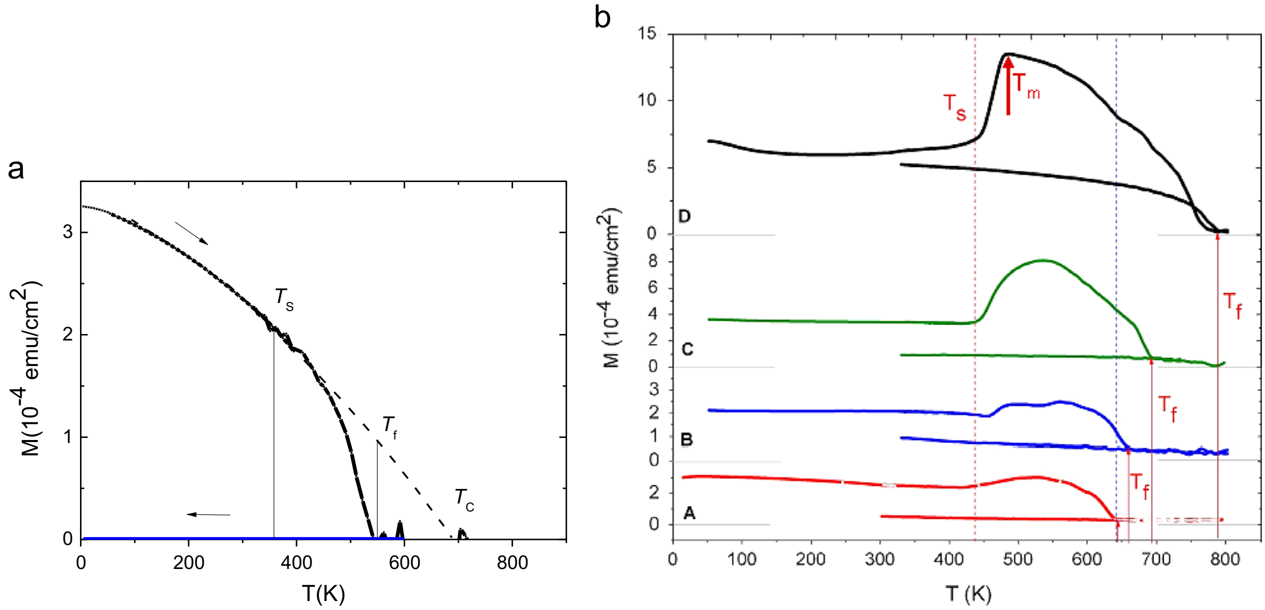

Fig. 1. The magnetization M(T) as a function of temperature: (a) of Type A sample Si(111)/SiO$_2$/[Fe(1.2)/Si(1.5 nm)]$_2$/[Fe(1.2)/Si(10 nm)]. (b) Type B samples (described in the text). T_S is the onset temperature of the irreversible formation of silicides, T_m is the temperature of maximum $M(T)$, and T_f is the end temperature of complete transformation.

spectroscopy (EELS) scanning transmission electron microscopy (STEM), performed on a focused ion beam (FIB)-cut crossection of the multilayer, allowed to confirm qualitatively the geometry of the sample [38]. X-ray reflectivity (XRR) was measured using synchrotron radiation allowing an in-depth probing of the multilayer. It was found that a protective SiO_2 external film formed upon exposure of the sample to air, however enough pure Si remained to determine the Si-on-Fe interface. The interface thickness amounts to 1.4(1) nm, with a roughness of 0.6(1) nm. These values are in good agreement with the total interface and roughness determined by small-angle X-ray scattering (SAXS) on Type A samples; Si(100)/[Fe(5 nm)/Si(1 nm)$]_2$)/[Fe(5 nm)/Si(10 nm)], and Si(111)/Fe(2 nm)/Si(2 nm)/Fe(10 nm)/Si(10 nm) [33].

The average density of the interface determined from the XRR experiment did not allow to assure the composition of the interface. To study the SiO_2/Si superficial layers [38,39] we employed angle resolved X-ray photoelectron spectroscopy (ARXPS) at fixed photon energy at the Si 2p and Fe 2p edges. The Si 2p spectral features could be explained to be caused by Si^{4+} from SiO_2, and other SiO_x suboxides. The Si^0 $2p_{1/2}$ peak can be assigned either to pure Si or to an Fe silicide. In fact, the dependence of the Si^0 $2p_{1/2}$ and Si^0 $2p_{3/2}$ peaks intensity ratio is observed to increase beyond the ½ ratio for a single Si species for decreasing emission angle (increasing probing depth); i.e. the Fe silicide is reached in this experiment. A deeper probing depth is achieved with hard X-ray photoelectron spectroscopy (HAXPES), at fixed angle and increasing photon energy of the synchrotron beam. With this technique we could reach clearly the Si-on-Fe interface and the Fe layer below. At the Si 1s spectra the S^0 1s core level peak and the peak shifted by $+4.5$ eV corresponding to the SiO_2 were identified. The Fe silicide imprint was associated to a pre-peak shifted -3.5 eV from the Si^0 1s and the -5 eV from the Fe^0 1s peaks, which could be explained as an interface effect. The results were quite compatible with the ARXPS experiment. However, the composition of the interlayer could not be assured with those techniques.

To achieve this goal, CEMS experiments were performed on samples designed for this purpose. A thin layer of ^{57}Fe isotope was deposited at the depths of interest, while for the rest of the Fe film ^{56}Fe, silent to the Mössbauer effect, was used. Thus the CEMS signal is given by the ^{57}Fe nuclei once the Fe silicides are formed. A reference sample was produced with the sequence Si(100)/SiO_2 /Si(6 nm)/[^{56}Fe(5 nm)/^{57}Fe(0.6 nm)/^{56}Fe(5 nm)/Si(6 nm)$]_3$ with the ^{57}Fe isotope in the middle of the Fe layer, which showed neatly a sextet due to α-Fe in a magnetic field parallel to the substrate. To study the Si-on-Fe and the Fe-on-Si interfaces two samples were fabricated, Si(100)/SiO_2/[^{56}Fe(9.4 nm)/^{57}Fe(0.6 nm)/Si(6 nm)$]_3$ and Si(100)/SiO_2/Si(6 nm)[^{57}Fe(0.6 nm)/^{56}Fe(9.4 nm)/Si(6 nm)$]_3$, respectively, Three Fe/Si layers were deposited to optimize the CEMS signal [38]. It is important to note that each Fe layer thickness (10 nm) is thick enough to guarantee that the Fe-on-Si and the Si-on-Fe interfaces do not mix, as is proven by the spectrum of the sample with the isotopic probe in the middle of the Fe layer that detects only α-Fe. The spectra of the other two samples showed systematically a paramagnetic doublet and complex structure of overlapping sextets that were analyzed using the multiple sextets method (see Fig. 2 left). In this method the sextet intensities are proportional to the Fe site environment probabilities and the hyperfine values are determined by the number of nearest neighbors. It was found that in both Fe-on-Si and Si-on-Fe interfaces a paramagnetic component, identified as c-$Fe_{1-x}Si$, was present in the same amount; i.e. this component is symmetric. In contrast, up to five different components were assigned to Fe nuclei with different number of neighbors: The Si-on-Fe interface is compatible with the presence of $Fe_{1-x}Si_x$, with x in the range 0.18–0.20, while the Fe-on-Si interface, narrower than the former, contains $Fe_{1-x}Si_x$, with $x \leq 0.18$. Therefore, we claim that the asymmetry in the composition is caused solely by the ferromagnetic components in the interfaces. When Fe is deposited on Si the paramagnetic phase is formed and a thin ferromagnetic $Fe_{1-x}Si_x$ develops, while when Si is deposited on Fe the $Fe_{1-x}Si_x$, with high Si content, is formed and subsequently the paramagnetic c-$Fe_{1-x}Si$ appears. Our results are compatible but

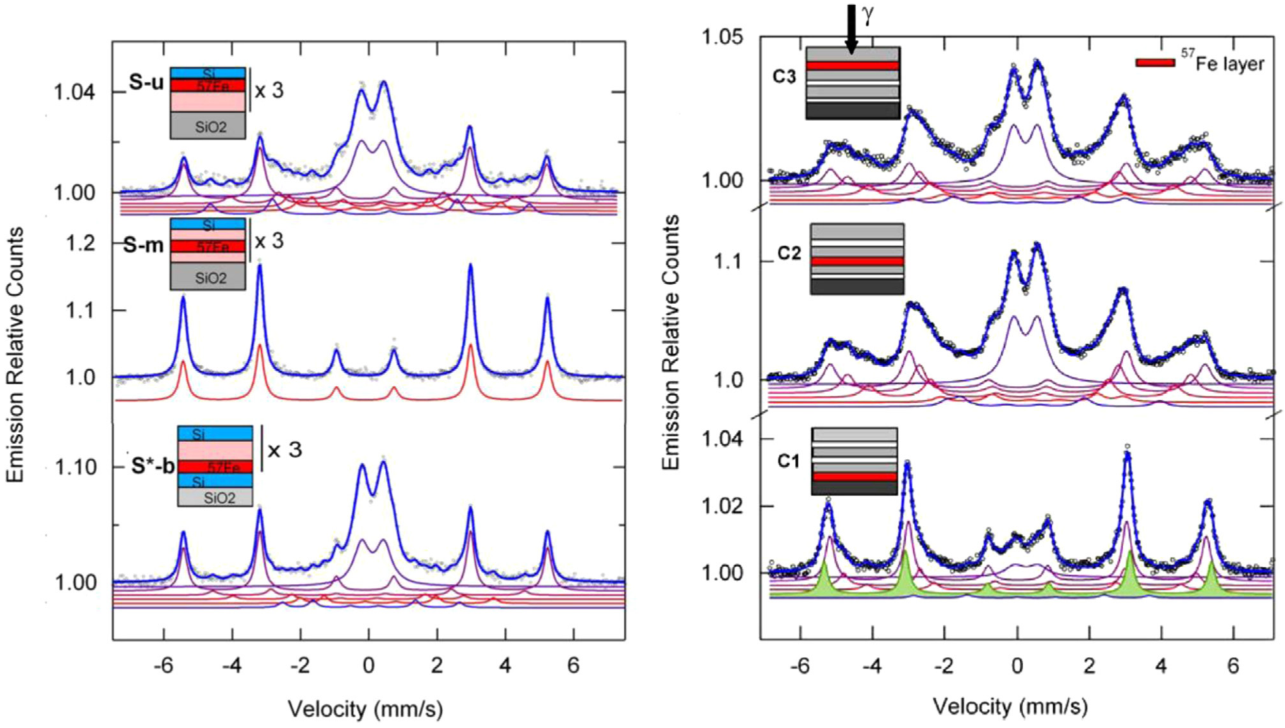

Fig. 2. CEMS spectra at room temperature of: (left) Type A samples; (right) Type B samples. The position of the ^{57}Fe isotopic probe is indicated in the insets in red. (For interpretation of the references to color in this figure legend, the reader is referred to the web version of this article.)

differ in detail with the asymmetry in interface compositions found earlier [17,26,39,40].

An independent X-ray magnetic circular dichroism (XMCD) experiment of similar samples was interpreted in terms of a continuous solution of $Fe_{1-x}Si_x$, from Fe_3Si to α-Fe and a paramagnetic component [41]. These authors also found an asymmetry of the compositions of both interfaces, although the actual thicknesses deduced were somewhat smaller than the present results.

Upon annealing the diffusion of Si in Fe was also clearly observed with the CEMS technique as the clean α-Fe in the middle position was seen to evolve to a mixed silicide composition and become fully paramagnetic at 600 K [42].

2.2. *Type B samples*

These multilayers were deposited on a previously fabricated substrate of GaAs/Fe(1 nm)/Ag(150 nm) [43]. Therefore, the Fe/Si bilayers deposited on top rested on a first Ag(100) layer that is immiscible with Fe, a fact that has a bearing on our results. Three samples were fabricated with different thicknesses of the Fe layers, but nominally identical to some of Type A samples, for comparison's sake GaAs/Fe(1 nm)/Ag(150 nm)[Fe(x)/Si(1.5 nm)$]_2$/Fe(x)/Si (10 nm)], with $x=1.2$, 1.6, 2.6 and 3.8 nm. The HAADF-STEM and high resolution HRTEM microscopy of a cross-section sample showed the formation of the three Fe/Si bilayers with FeSi interfaces. Magnetization hysteresis measurements evidence the reduction of saturation magnetization in the as-prepared samples caused by the formation of non-magnetic Fe silicides during the deposition of the layers at room temperature, in good accordance with the same effect found in Type A samples. L-MOKE images as a function of a variable magnetic field parallel to the films allowed observing the formation of magnetic domains with a small anisotropy.

However, it was quite surprising to find that when annealing above 400 K the $M(T)$ curve showed an upturn to a maximum, for which its temperature T_m and height depended on the Fe layer thickness, while for increasing temperature a decay till disappearance of any ferromagnetic component takes place (see Fig. 1 right). This process is irreversible in temperature. This feature is completely different than the M(T) curves of Type A samples. The increase in magnetization upon heating is caused by the reaction of Fe and Si transforming the paramagnetic c-$Fe_{1-x}Si$ phase existing in the interfaces towards Fe silicides with a larger Fe content, probably Fe_3Si. When all available Fe has reacted the process stops and upon further heating there is a transformation to paramagnetic phases. The difference in height and T_m of the maximum increase with the Fe layer thickness since the Fe layers constitute the Fe reservoir for the chemical process. It is obvious that the difference of M(T) behavior between Type A and B samples originates in the preparation process. In Type A the first Fe layer is deposited on Si or SiO_2, therefore there is a reservoir of Si to react into the paramagnetic c-$Fe_{1-x}Si$, while in Type B it is deposited on Ag that does not provide that excess in Si. Therefore the reaction drives towards rich Fe silicides.

The composition of the Fe layers as deposited was determined by means of CEMS on three identical samples GaAs/Fe(1 nm)/Ag (150 nm)[Fe(2.6 nm)/Si(1.5 nm)$]_2$/Fe(2.6)/Si(10 nm)], where each sample contained only one out of the three layers formed by ^{57}Fe [43] (see Fig. 2 right). The spectra with ^{57}Fe in the top-most layer and in the middle one are similar, but that of the ^{57}Fe layer directly deposited on Ag is very different. Using the same analysis technique of the spectra as described in the previous section it was found that the latter case, Fe grows on Ag epitaxially and α-Fe is present, while it is absent in the other two layers. In fact, in the bottom layer there is just one Si-on-Fe interface while the other two layers have a Si-on-Fe and a Fe-on-Si interface. The paramagnetic phase c-$Fe_{1-x}Si$, identified from the doublet feature, is present in all three layers, but its intensity is double in the top-most and middle ^{57}Fe layer than in that deposited on Ag. Therefore, we conclude that, as in the Type A samples, the paramagnetic phase is symmetric and characteristic in all the Fe–Si interfaces, and is assigned to defective/strained c-$Fe_{1-x}Si$ phase. In contrast, the composition of the ferromagnetic silicides present in the top-most and middle ^{57}Fe layers is qualitatively similar since the percentage amount of the $Fe_{1-x}Si_x$ ferromagnetic phases, with $x\approx 0.15$, is 70% in the top-most ^{57}Fe layer and 67% in the middle one.

3. Conclusions

The $(Fe/Si)_n$ multilayers fabricated by MBE on either Si wafers or Ag(100) buffer layers form interfaces, with a width of 1.4 nm and a roughness of 0.6 nm. During the sample fabrication Fe silicides are formed at the interfaces that have as an effect the reduction of saturation magnetization of the sample with decreasing Fe film thickness.

The multilayers have in common symmetric (Fe-on-Si and Si-on-Fe) paramagnetic c-$Fe_{1-x}Si$ phase adjacent to the Si layer (if there remains any pure Si). However, in both interfaces there is an inhomogeneous ferromagnetic component of general formula $Fe_{1-x}Si_x$ with x ranging in composition from $x\le 0.15$ to a maximum of $x=0.2$. The thermal stability of these multilayers remains till 400 K. Above this temperature chemical reactions take place that modify the interface compositions depending on the available Fe and Si in the sample till a non-magnetic phase at temperature of the order of 700–800 K.

Acknowledgments

The financial support of the Spanish MINECO MAT2011-23791 and MAT2015-53921-R, Aragonese DGA-IMANA E34 (cofounded by Fondo Social Europeo) and European FEDER funds is acknowledged. Program of the President of the Russian Federation for the support of leading scientific schools (Scientific School 2886.2014.2), RFBR (Grant no. 13-02-01265), the Ministry of Education and Science of the Russian Federation (State contract no. 02. G25.31.0043 and State task no. 16.663.2014K)

References

[1] M.N. Baibich, J.M. Broto, A. Fert, F.N. Van Dau, F. Petroff, P. Eitenne, et al., Giant magnetosresistance of (001)Fe/(001)Cr magnetic superlattices, Phys. Rev. Lett. 61 (1988) 2472–2475, http://dx.doi.org/10.1103/PhysRevLett.61.2472.

[2] G. Binasch, P. Grünberg, F. Saurenbach, W. Zinn, Enhanced magnetoresistance in layered magnetic structures with antiferromagnetic interlayer exchange, Phys. Rev. B 39 (1989) 4828–4830, http://dx.doi.org/10.1103/PhysRevB.39.4828.

[3] R.R. Gareev, D.E. Bürgler, M. Buchmeier, D. Olligs, R. Schreiber, P. Grünberg, Metallic-type oscillatory interlayer exchange coupling across an epitaxial FeSi spacer, Phys. Rev. Lett. 87 (2001) 157202, http://dx.doi.org/10.1103/PhysRevLett.87.157202.

[4] G. Strijkers, J. Kohlhepp, H. Swagten, W. de Jonge, Origin of biquadratic exchange in Fe/Si/Fe, Phys. Rev. Lett. 84 (2000) 1812–1815, http://dx.doi.org/10.1103/PhysRevLett.84.1812.

[5] S. Datta, B. Das, Electronic analog of the electro-optic modulator, Appl. Phys. Lett. 56 (1990) 665–667, http://dx.doi.org/10.1063/1.102730.

[6] S.A. Wolf, D.D. Awschalom, R.A. Buhrman, J.M. Daughton, S. von Molnár, M. L. Roukes, et al., Spintronics: a spin-based electronics vision for the future, Science 294 (2001) 1488–1495, http://dx.doi.org/10.1126/science.1065389.

[7] J. Barnas, A. Fuss, R.E. Camley, P. Grünberg, W. Zinn, Novel magnetoresistance effect in layered magnetic structures: theory and experiment, Phys. Rev. B 42 (1990) 8110–8120, http://dx.doi.org/10.1103/PhysRevB.42.8110.

[8] P. Grünberg, R. Schreiber, Y. Pang, U. Walz, M.B. Brodsky, H. Sowers, Layered magnetic structures: evidence for antiferromagnetic coupling of Fe layers

across Cr interlayers, Phys. Rev. Lett. 57 (1986) 8110–8120, http://dx.doi.org/10.1063/1.338656.

[9] S. Toscano, B. Briner, H. Hopster, M. Landolt, Exchange-coupling between ferromagnets through a non-metallic amorphous spacer-layer, J. Magn. Magn. Mater. 114 (1992) L6–L10, http://dx.doi.org/10.1016/0304-8853(92)90326-J.

[10] E.E. Fullerton, J.E. Mattson, S.R. Lee, C.H. Sowers, Y.Y. Huang, G. Felcher, et al., Non-oscillatory antiferromagnetic coupling in sputtered Fe/Si supperlattices, J. Magn. Magn. Mater. (1992) L301–L306.

[11] R.R. Gareev, D.E. Bürgler, M. Buchmeier, R. Schreiber, P. Grünberg, Very strong interlayer exchange coupling in epitaxial Fe/Fe$_{1-x}$Si$_x$/Fe trilayers (x=0.4–1.0), J. Magn. Magn. Mater. 240 (2002) 235–237.

[12] J. de Vries, J. Kohlhepp, F. den Broeder, R. Coehoorn, R. Jungblut, A. Reinders, et al., Exponential Dependence of the interlayer exchange coupling on the spacer thickness in MBE-grown Fe/SiFe/Fe sandwiches, Phys. Rev. Lett. 78 (1997) 3023–3026, http://dx.doi.org/10.1103/PhysRevLett.78.3023.

[13] Q.G. Zhu, H. Iwasaki, E.D. Williams, R.L. Park, Formation of iron silicide thin films, J. Appl. Phys. 60 (1986) 2629–2631, http://dx.doi.org/10.1063/1.337136.

[14] H.F. Hsu, H.Y. Wu, Y.T. Huang, T.H. Chen, Structural properties of iron silicide nanostructures grown by reactive deposition epitaxy, Jpn. J. Appl. Phys. 48 (2009) 1–5, http://dx.doi.org/10.1143/JJAP.48.08JB09.

[15] M. De Crescenzi, G. Gaggiotti, N. Motta, F. Patella, A. Balzarotti, Bremsstrahlung-isochromat-spectroscopy and x-ray-photoelectron-spectroscopy investigation of the electronic structure of β-FeSi$_2$ and the Fe/Si(111) interface, Phys. Rev. B 42 (1990) 5871, http://dx.doi.org/10.1103/PhysRevB.42.5871.

[16] J.M. Gallego, R. Miranda, The Fe/Si(100) interface, J. Appl. Phys. 69 (1991) 1377–1383.

[17] G. Strijkers, J. Kohlhepp, H. Swagten, W. Jonge, Formation of nonmagnetic c-Fe$_{1-x}$Si in antiferromagnetically coupled epitaxial Fe/Si/Fe, Phys. Rev. B 60 (1999) 9583–9587, http://dx.doi.org/10.1103/PhysRevB.60.9583.

[18] K. Konuma, J. Vrijmoeth, P.M. Zagwijn, E. Vlieg, J.F. van der Veen, Formation of ironsilicide on Si(001), Appl. Surf. Sci. 70–71 (1993) 564–568, http://dx.doi.org/10.1016/0169-4332(93)90580-5.

[19] A. Gupta, D. Kumar, V. Phatak, Asymmetric diffusion at the interfaces in Fe/Si multilayers, Phys. Rev. B: Condens. Matter Mater. Phys. 81 (2010) 155402, http://dx.doi.org/10.1103/PhysRevB.81.155402.

[20] E.V. Chubunova, I.D. Khabelashvili, Y.Y. Lebedinskii, V.N. Nevolin, A. Zenkevich, Direct observation of silicide growth at FeSi interface during pulsed laser deposition, Thin Solid Films 247 (1994) 39–43, http://dx.doi.org/10.1016/0040-6090(94)90473-1.

[21] G. Crecelius, Reaction of iron on silicon, Appl. Surf. Sci. 65–66 (1993) 683–689, http://dx.doi.org/10.1016/0169-4332(93)90739-X.

[22] R. Kläsges, C. Carbone, W. Eberhardt, C. Pampuch, O. Rader, T. Kachel, et al., Formation of a ferromagnetic silicide at the Fe/Si(100) interface, Phys. Rev. B 56 (1997) 10801–10804, http://dx.doi.org/10.1103/PhysRevB.56.10801.

[23] N. Cherief, J. Veuillen, T.A.N. Tan, R. Cinti, J. Derrien, Formation of the Fe-stepped Si(100) interface as studied by electron spectroscopy, Vacuum 41 (1990) 1350–1352, http://dx.doi.org/10.1016/0042-207X(90)93954-H.

[24] J.M. Gallego, J.M. Garcia, J. Alvarez, R. Miranda, Metasllization-induced spontaneous formation at room temperature: the Fe/Si case, Phys. Rev. B. 46 (1992) 13339.

[25] M.V. Gomoyunova, D.E. Malygin, I.I. Pronin, a S. Voronchikhin, D.V. Vyalikh, S. L. Molodtsov, Initial stages of iron silicide formation on the Si(100)2 × 1 surface, Surf. Sci. 601 (2007) 5069–5076, http://dx.doi.org/10.1016/j.susc.2007.09.007.

[26] S.R. Naik, S. Rai, M.K. Tiwari, G.S. Lodha, Structural asymmetry of Si/Fe and Fe/Si interface in Fe/Si multilayers, J. Phys. D: Appl. Phys. 41 (2008) 115307, http://dx.doi.org/10.1088/0022-3727/41/11/115307.

[27] S.R. Naik, S. Rai, G.S. Lodha, R. Brajpuriya, X-ray reflectivity and photoelectron spectroscopy study of interdiffusion at the Si/Fe interface, J. Appl. Phys. 100 (2006) 1–6, http://dx.doi.org/10.1063/1.2210168.

[28] A. Chaiken, R.P. Michel, M.A. Wall, Structure and magnetism of Fe/Si multilayers grown by ion-beam sputtering, Phys. Rev. B 53 (1996) 5518–5529, http://dx.doi.org/10.1103/PhysRevB.53.5518.

[29] L. Thanh Vinh, J. Chevrier, J. Derrien, Epitaxial growth of Fe–Si compounds on the silicon (111) face, Phys. Rev. B 46 (1992) 15946.

[30] S.N. Varnakov, A.S. Parshin, S.G. Ovchinnikov, D. Rafaja, L. Kalvoda, A.D. Balaev, et al., Structural and magnetic characteristics of Fe/Si bilayer and multilayer films obtained by thermal deposition in ultrahigh vacuum, Tech. Phys. Lett. 31 (2005) 947, http://dx.doi.org/10.1134/1.2136961.

[31] S.N. Varnakov, A.A. Lepeshev, S.G. Ovchinnikov, A.S. Parshin, M.M. Korshunov, P. Nevoral, Automation of technological equipment for obtaining multilayer structures in an ultrahigh vacuum, Instrum. Exp. Tech. 47 (2004) 839–843, http://dx.doi.org/10.1023/B:INET.0000049709.08368.3e.

[32] D.E. Bürgler, C.M. Schmidt, J.A. Wolf, T.M. Schaub, H.J. Güntherodt, Ag films on Fe/GaAs(001): from clean surfaces to atomic Ga structures, Surf. Sci. 366 (1996) 295–305, http://dx.doi.org/10.1016/0039-6028(96)00825-4.

[33] A.S. Parshin, S.N. Varnakov, A.A. Lepeshev, D. Rafaja, L. Kalvoda, S. G. Ovchinnikov, Characterization of Si/Fe multilayers by electron spectroscopy and small-angle X-ray scattering, Phys. Met. Metallogr. 101 (2006) S78–S80, http://dx.doi.org/10.1134/S0031918X06130230.

[34] S.N. Varnakov, J. Bartolomé, J. Sesé, S.G. Ovchinnikov, S.V. Komogortsev, A. S. Parshin, et al., Size effects and magnetization of (Fe/Si)$_n$ multilayer film nanostructures, Phys. Solid State 49 (2007) 1470–1475, http://dx.doi.org/10.1134/S1063783407080124.

[35] S.N. Varnakov, S.V. Komogortsev, S.G. Ovchinnikov, J. Bartolomé, J. Sesé, Magnetic properties and nonmagnetic phases formation in (Fe/Si)$_n$ films, J. Appl. Phys. 104 (2008) 094703, http://dx.doi.org/10.1063/1.3005973.

[36] S.M. Zharkov, R.R. Altunin, E.T. Moiseenko, G.M. Zeer, S.N. Varnakov, S. G. Ovchinnikov, Solid-state reactions in Fe/Si multilayer nanofilms, Solid State Phenom. 215 (2014) 144–149, http://dx.doi.org/10.4028/www.scientific.net/SSP.215.

[37] S.V. Komogortsev, S.N. Varnakov, S.A. Satsuk, I.A. Yakovlev, S.G. Ovchinnikov, Magnetic anisotropy in Fe films deposited on SiO$_2$/Si(001) and Si(001) substrates, J. Magn. Magn. Mater. 351 (2014) 104–108, http://dx.doi.org/10.1016/j.jmmm.2013.09.058.

[38] L. Badía-Romano, J. Rubín, F. Bartolomé, C. Magén, J. Bartolomé, S.N. Varnakov, et al., Morphology of the asymmetric iron–silicon interfaces, J. Alloy. Compd. 627 (2015) 136–145, http://dx.doi.org/10.1016/j.jallcom.2014.12.019.

[39] L. Badía-Romano, J. Rubín, F. Bartolomé, J. Bartolomé, S. Ovchinnikov, S. Varnakov, et al., Morphological and compositional study at the Si/Fe interface of (Fe/Si) multilayer, Spin 4 (2014) 1440002, http://dx.doi.org/10.1142/S2010324714400025.

[40] A. Gupta, D. Kumar, V. Phatak, Asymmetric diffusion at the interfaces in Fe/Si multilayers, Phys. Rev. B: Condens. Matter Mater. Phys. 81 (2010) 1–5, http://dx.doi.org/10.1103/PhysRevB.81.155402.

[41] M.S. Platunov, S.N. Varnakov, S.M. Zharkov, G.V. Bondarenko, E. Weschke, E. Schierle, et al., Analysis of the structure and magnetic properties of an interface in multilayered (Fe/Si)$_N$ nanostructures with the surface-sensitive XMCD method, JETP Lett. 99 (2014) 706–711, http://dx.doi.org/10.1134/S002136401412011X.

[42] S.N. Varnakov, S.G. Ovchinnikov, J. Bartolomé, J. Rubín, L. Badía, G. V. Bondarenko, CEMS analysis of phase formation in nanostructured films (Fe/Si)$_3$, Solid State Phenom. 168–169 (2010) 277–280, http://dx.doi.org/10.4028/www.scientific.net/SSP.168-169.277.

[43] L. Badía-Romano, J. Rubín, C. Magén, D.E. Bürgler, J. Bartolomé, Iron silicide formation at different layers of (Fe/Si)$_3$ multilayered structures determined by conversion electron Mössbauer spectroscopy, J. Appl. Phys. 116 (2014) 023907-1-6, http://dx.doi.org/10.1063/1.4887522.